



Controlling physiological angiogenesis by hypoxia-induced signaling

E. Hadjipanayi^a, R.A. Brown^{a,*}, V. Mudera^a, D. Deng^b, W. Liu^b, U. Cheema^a

^a UCL Division of Surgery and Interventional Sciences, Tissue Repair and Engineering Centre, Brockley Hill, Stanmore Campus, London, HA7 4LP, UK

^b Department of Plastic and Reconstructive Surgery, Ninth People's Hospital and Tissue Engineering Center, Shanghai, JiaoTong University School of Medicine, Shanghai, PR China

ARTICLE INFO

Article history:

Received 18 February 2010

Accepted 30 May 2010

Available online 9 June 2010

Keywords:

Vascularization
Angiogenic factors
Cell-based therapy
Depot-release
Biomimetic
Collagen

ABSTRACT

The full sequence of signals leading to new blood vessel formation is a physiological response to tissue hypoxia through upregulation of angiogenic factor cascades. Controlled initiation of this mechanism for therapeutic/engineered angiogenesis must rely on precisely localized hypoxia. Here we have designed a 3D *in vitro* model able to test the effect and predictability of spatially positioned local hypoxic stimuli using defined cell depots within a 3D collagen matrix. Cell-mediated hypoxia was engineered using human dermal fibroblasts (HDFs), to generate a local population of Hypoxia-Induced Signaling (HIS) cells. HIS cell depots released angiogenic factors which induced directional endothelial cell (EC) migration and tubule formation in a spatially defined assay system. Non-hypoxic baseline control cultures induced minimal EC migration with little tubule formation. Furthermore, depots of HIS cells, positioned in the core of 3D collagen constructs directed host vessel in-growth deep into the implant by 1 week, which was at least 7 days earlier than in non-hypoxia pre-conditioned constructs. The functionality of *in vivo* vascularisation was verified by real-time monitoring of O₂ levels in the core of implanted constructs. These findings establish the angiogenic potential of HIS cells applicable to *in vitro* tissue modeling, implant vascularization and engineering predictable angiogenic therapies.

© 2010 Elsevier B.V. All rights reserved.

1. Introduction

It is becoming clear that changing local O₂ tension can affect multiple aspects of cell phenotype and behavior, including proliferation and differentiation [1–3]. Mammalian tissues operate in oxygen tensions ranging from 1 to 10% O₂ (pO₂ between 7.6 and 76 mm Hg) [4], termed physiological hypoxia. This range is distinct from 'pathological' hypoxia (<1% O₂ or <7.6 mm Hg), where O₂ tension is low enough to compromise cell metabolism and damage/kill cells. Culturing cells under physiological hypoxia is currently employed as a strategy to control cell behavior *in vitro*, in particular, up-regulating the production of angiogenic signaling molecules [5,6].

As O₂ tension drops in a tissue, cells primarily respond by up-regulating Hypoxia Inducible Factor 1 alpha (HIF-1α), which is a transcriptional activator [7]. HIF-1α is considered to act as a regulator of O₂ by controlling cell production of potent angiogenic proteins, for example vascular endothelial growth factor (VEGF) [7]. Angiogenesis *in vivo* relies upon gradients of angiogenic factors guiding endothelial cells, and ultimately vessels, to tissue areas where O₂ and nutrients are required [8–10]. Reproducing these complex angiogenic factor gradients within a tissue construct, by engineering hypoxia in a convenient cell type, would have huge therapeutic and experimental value. The idea would be to induce cells to act as factories producing a

cascade of angiogenic proteins that can generate a physiological angiogenic response on demand. Additionally, the ability to induce controllable cell-mediated, and therefore physiologically regulated hypoxia [11] at predictable spatial locations in tissues would make it possible to direct the angiogenic response to any chosen point in 3D.

It is well documented that cell-generated angiogenic cascades (following prolonged exposure to reduced O₂) result in a more functional vasculature. This is almost certainly because the component proteins work best in concert to orchestrate vessel formation [12,13]. Simple addition of unbalanced levels of single factors such as VEGF has been shown to result in the formation of non-functional, 'leaky' vessels [12]. Consequently, it is proposed here that well-orchestrated biomimetic production of angiogenic factors with feedback regulation (angiogenic engineering) is only likely to be a practical proposition using whole cell systems. By these means the need to reproduce a complex sequence of angiogenic proteins is conveniently avoided by harnessing the innate biological programming. This can be achieved by engineering controlled cell hypoxia, i.e. mimicking physiological tissue hypoxia, which automatically elicits physiological angiogenesis in the body [10,14].

A major advantage in the use of scaffolds for tissue fabrication is the potential to control cellular micro-environments by customizing parameters such as diffusive properties and cell densities [5,15]. Previous work by this group has shown that high density seeding of 3D collagen constructs with human dermal fibroblasts (HDFs) produced rapid reductions of core O₂ tension (~25 mm Hg/3.2%), i.e. at the low end of physiological hypoxia [5]. Importantly, this

* Corresponding author. Tel.: +44 20 8909 5845; fax: +44 20 8954 8560.
E-mail address: rehkrab@ucl.ac.uk (R.A. Brown).

elicited a multifold up-regulation of VEGF gene expression up to 8 days, in a spatially predictable manner, with highest expression in the core vs. mid and surface layers [5]. In contrast to other studies where cells are incubated in a low O₂ atmosphere, i.e. exposed to locally-uncontrolled, global hypoxia [16–20], cell hypoxia in the present model is created by cell O₂ consumption. By controlling the seeding cell type, density and position, therefore the total cell-depot O₂ consumption, it is possible to define accurately where the hypoxia will develop within a 3D construct (i.e. core O₂<surface O₂) [5]. This makes it possible to engineer distinct populations of Hypoxia-Induced Signaling (HIS) cells that function independently of other cell populations, such as responding endothelial cells (ECs).

In this study we tested the hypothesis that 3D co-culture of a HIS cell population (HDFs) with ECs (HUVECs), would rapidly induce a physiological angiogenic response. In this 3D *in vitro* model the directing HIS cells (hypoxic HDFs) and the responding cells (ECs) could be spatially positioned to prevent initial direct cell contact. HDFs were either exposed to normoxia (incubator levels) or localized physiological hypoxia to up-regulate critical angiogenic factors (HIF-1 α , VEGF). *In vitro* bioresponse was monitored in terms of EC migration and tube formation towards the angiogenic factor source (HIS cells). The practical effectiveness of spatially controlled hypoxia-induced signaling to promote and direct vascularisation *in vivo* was then tested by implanting collagen constructs, incorporating HIS cell depots in their core, subcutaneously and intramuscularly in rabbits. The effect of pre-conditioning constructs prior implantation, to optimize up-regulation of angiogenic signaling, was assessed using specific EC staining, while the functionality of newly formed vessels was assessed by extended real-time O₂ monitoring.

2. Materials and methods

2.1. Cell culture

Adult human dermal fibroblasts (HDFs) and male New Zealand white rabbit dermal fibroblasts (RDFs) were cultivated in DMEM supplemented with 10% FCS (First Link, UK), 1000 U/ml penicillin and 100 mg/ml streptomycin (Gibco, UK). Human umbilical vein endothelial cells (HUVECs) were cultured in complete endothelial cell growth medium (Promo Cell, Germany).

2.2. Scaffold fabrication and culture

HDF-, HUVEC- and RDF-seeded rat-tail type I collagen gels were prepared as previously described [21] (see [Supplementary methods section](#) for preparation of HDF/HUVEC co-seeded and RDF-seeded constructs). HDF/HUVEC co-seeded constructs were either cultured as flat sheets (sheet co-culture) or spiralled to axially align the HDF and HUVEC compartments (axial co-culture) or to position the HDF compartment in the core and the HUVEC compartment on the surface (radial co-culture) (Fig. 1A). RDF-seeded spiral constructs comprised of a cellular core and an acellular wrap (Fig. 4B). HDFs and RDFs in spiral constructs were referred to as HIS-HDFs and HIS-RDFs, respectively, to indicate their function as hypoxia-induced signaling (HIS) cells. For *in vitro* experiments, constructs were cultured statically in 5 ml medium (50% DMEM, 50% endothelial growth medium) in a 37 °C, 5% CO₂ humidified incubator for the time indicated. Axial HDF/HUVEC co-cultures were also cultured in the presence of anti-VEGF neutralizing

IgG (R&D, USA) at saturating concentration (10 μ g/ml) [20] or control goat IgG (10 μ g/ml) (Sigma, UK) for 1 week. For *in vivo* experiments, RDF-seeded constructs were either cultured *in vitro* in 5 ml fully supplemented DMEM for 5 days prior to implantation (pre-conditioning) or implanted immediately (no pre-conditioning). Four replicate constructs were used to test each condition.

ELISA. See [Supplementary methods section](#).

2.3. Implantation of collagen constructs

2.3.1. Subcutaneous implantations

An institutional review committee of Shanghai Second Medical University approved all animal study protocols. Twelve adult female New Zealand white rabbits (2–2.5 kg) were used. Surgery was performed under general anaesthesia. A longitudinal skin incision was made on the rabbit's back and implants were sutured onto subcutaneous tissue. Three acellular constructs were sutured onto the left side and three cellular constructs (of the same series) on the right. Cell densities were either low (5.8×10^6 RDFs/ml) or high (23.2×10^6 RDFs/ml) with pre-conditioning and high (23.2×10^6 RDFs/ml) cell density with no pre-conditioning. Rabbits were nursed until full recovery and returned to their single cage. Rabbits were sacrificed at 1 and 2 weeks. There were six rabbits in each of the 1-week and 2-week groups allowing testing of 6 constructs per condition for each implantation period.

2.3.2. Intramuscular implantations

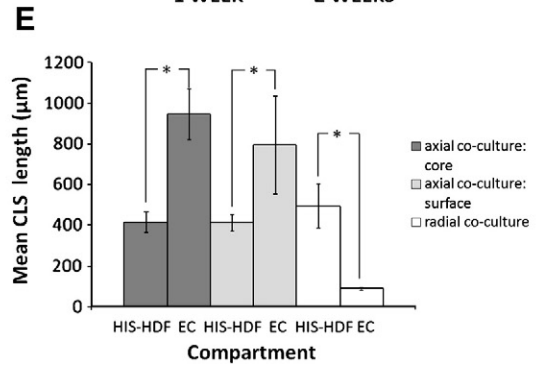
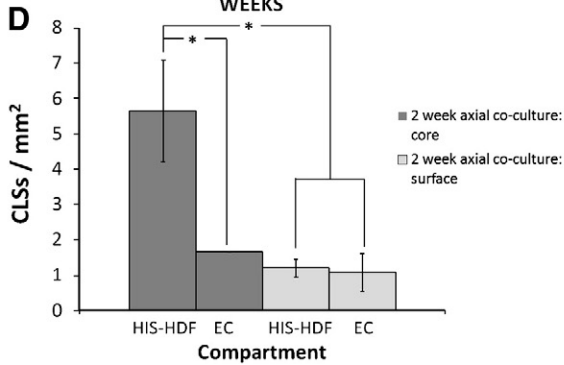
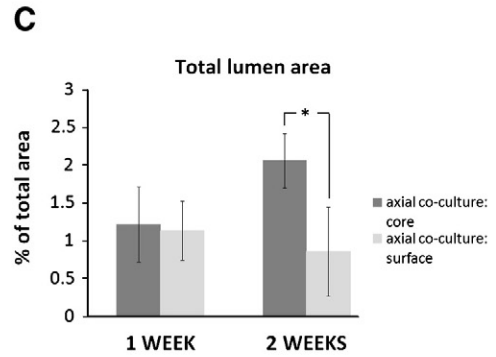
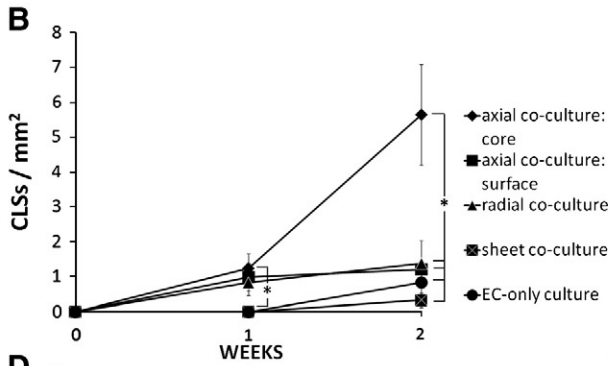
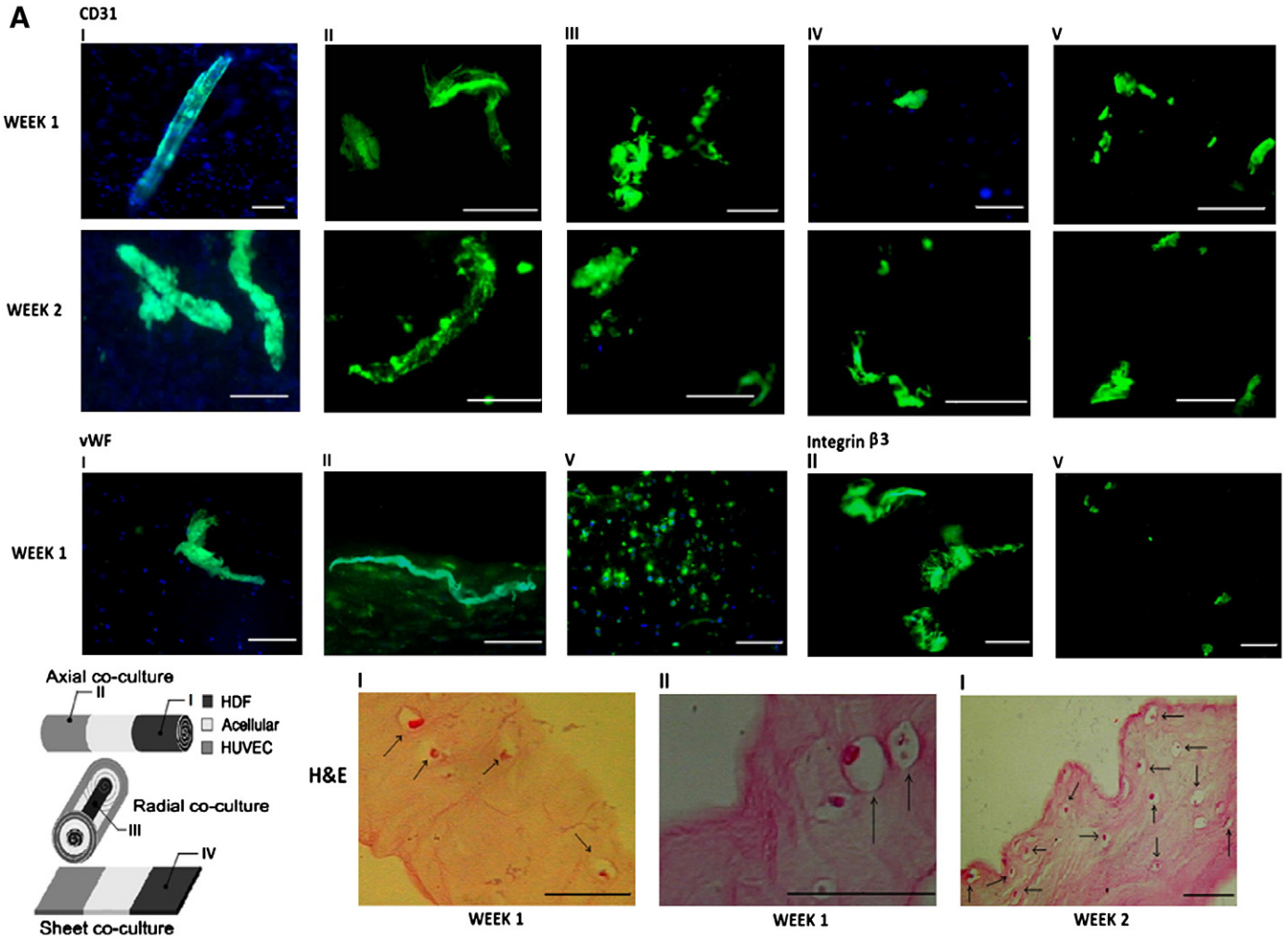
A longitudinal skin incision was made on the rabbit's back and a construct spiralled round a 0.9 mm diameter cannula was inserted into a pouch within the back muscles. The muscle and skin layers were closed with interrupted 3.0 sutures, such that the cannula's opening protruded through the skin. The cannulas were sealed with cotton wool to prevent atmospheric exposure. One construct was implanted per rabbit with three rabbits used to test each condition; acellular, low (5.8×10^6 RDFs/ml) and high (23.2×10^6 RDFs/ml) cell density constructs (no pre-conditioning). A fibre-optic O₂ probe (Oxford Optronix Ltd, Oxford, UK) was inserted into the cannula of each rabbit to monitor core O₂ tension (see [Supplementary methods section](#) for *in vivo* oxygen monitoring). The rabbits were sacrificed at 2 weeks.

Tissue processing and Immunohistochemical staining. See [Supplementary methods section](#).

2.4. Image analysis

An imaging software (Image J, NIH, USA) was used to determine the area of endothelial cell clusters (aggregates of >2 endothelial cells with an elongation index (ratio of major/minor axis) of <2), the length of capillary-like structures (CLSs), the CLS elongation index (ratio of straight line separation of CLS ends/total CLS length), the total lumen area, the total area of red blood cell (RBC)-containing lumens, host blood vessel invasion distance (average radial distance from construct edge where RBC-containing lumens were present) and the total field area. Total number of CLSs and endothelial cell clusters were counted manually. A minimum of 10 random fields were analysed per sample.

Fig. 1. Induction of *in vitro* angiogenesis by hypoxia-induced signalling (HIS). (A) Capillary-like structures (CLSs) and endothelial cell clusters (ECCs) in (I) core of HIS-HDF/EC axial co-cultures, (II) surface of HIS-HDF/EC axial co-cultures, (III) HIS-HDF/EC radial co-cultures, (IV) HDF/EC sheet co-cultures and (V) EC only-cultures at 1 and 2 weeks; visualised with human anti-CD31, anti-vWF, anti-integrin α v β 3 (green) and DAPI nuclear staining (blue) (bars = 200 μ m). H&E staining of HIS-HDF/EC axial co-cultures (cross-sections) showed CLS lumens (arrowed, bars = 100 μ m). Schematic indicates the region in the construct where images were taken for the three different co-cultures. (B) Quantification of CD31 +ve CLSs in the HDF compartment of different co-cultures and in EC-only cultures. (C) Comparison of core and surface total lumen area (H&E stained sections as % total section area) for HIS-HDF/EC axial co-cultures. (D) Comparison of CD31 +ve CLSs in HIS-HDF and EC compartments of axial co-cultures (core & surface) at 2 weeks. (E) Mean length of CD31 +ve CLSs in HIS-HDF and EC compartments of axial co-cultures (core & surface) and radial co-cultures at 2 weeks. For plots B, D, E bars correspond +/-se of means, for plot C bars correspond +/-sd of means, * p <0.05. Four constructs (n =4) were tested for each condition per time point.



2.5. Statistical analysis

For each experimental condition a sample size of 3 or more was used. Data is expressed as mean \pm standard deviation or mean \pm standard error, as noted. Statistical analysis was carried out using oneway ANOVA accompanied with multiple comparison tests, using SPSS 14 software. Differences were considered significant when $p < 0.05$ unless otherwise noted.

3. Results

3.1. In vitro induction of angiogenesis by hypoxia-induced signaling

HDFs and HUVECs were spatially positioned within sheet or spiral collagen constructs such that the two cell populations were separated by an acellular region (Fig. 1A). HDFs were seeded at high density (23.2×10^6 cells/ml) such that in spiral constructs (axial and radial models) cell O_2 consumption generated physiological hypoxia (~ 25 mm Hg/3.2% O_2) in the HDF compartment's core within 24 h [5]. In contrast, HDFs within sheet constructs (~ 200 μ m thick) were constantly exposed to near culture medium O_2 levels, i.e. non-hypoxia (140–160 mm Hg/18.4–21% O_2) [5].

We tested the hypothesis that co-culturing hypoxia-induced signaling HDFs (HIS-HDFs) with ECs (HUVECs), within 3D spiral constructs, would result in a physiological angiogenic response. In such HIS-HDF/EC co-cultures ECs formed CD31 and vWF positive endothelial cell clusters (ECCs) and capillary-like structures (CLSs) with lumens after 1 week (Fig. 1A). CLS formation in the HIS-HDF compartment indicated that ECs had migrated through the acellular region and invaded the HIS-HDF compartment by 1 week, suggesting that a functional angiogenic factor gradient was established from the HIS-HDFs towards the EC zone. In addition, CLSs in the EC compartment stained positively for integrin $\alpha v \beta 3$ (Fig. 1A), typical of migrating endothelial cells [22]. At 1 week all 3D spiral co-cultures (axial and radial models) had significantly greater CLS scores than non-hypoxic sheet co-cultures or EC-only culture controls ($p < 0.05$) (Fig. 1B). After 2 weeks only the core of axial co-cultures had significantly greater CLS density, by a factor of 5 to 10 fold depending on which zones/models were compared. Specifically, CLS density was ~ 6 fold higher in the core of axial co-cultures compared to the surface ($p < 0.05$) (Fig. 1B).

In HIS-HDF/EC co-cultures the spatial positioning of the two cell populations directly affected the pattern of angiogenesis. In axial model co-cultures there was a significant increase in the number of CLSs within the HIS-HDF compartment in the core, but not on the surface, from 1 to 2 weeks (Fig. 1B). A similar response was also seen for total lumen area, which increased from 1 to 2 weeks only in the core of axial co-cultures, in this case by ~ 2 fold (Fig. 1A,C). The number of CLSs in the HIS-HDF and EC compartments of axial co-cultures was the same at the construct surface, but ~ 3 fold greater within the core HIS-HDF compartment than in the core EC compartment, at 2 weeks ($p < 0.05$) (Fig. 1D). In contrast, radial model co-cultures produced a small CLS response at 1 week (same as axial model) but no increase in core CLS score from 1 to 2 weeks (Fig. 1B), consistent with the idea that the 3D growth factor diffusion barrier is also important.

Mean CLS length within the HIS-HDF compartment (both axial and radial models) did not significantly change between weeks 1 and 2 (data not shown). However, the 3D positioning of the HIS-HDF and EC populations did significantly influence CLS length at 2 weeks. In axial model co-cultures, CLS length was over 2 fold greater in the EC compartment compared to the HIS-HDF compartment (both core and surface: $p < 0.05$) (Fig. 1E). In complete contrast, CLS length in the radial co-culture model was 5 fold greater in the HIS-HDF compartment ($p < 0.05$) (Fig. 1E). CLS elongation index (ratio of straight line separation of CLS ends/total CLS length) in the HIS-HDF and EC

compartments was in the range of 0.8–1 for both culture models, indicating that longer CLSs were straight and directional, rather than tortuous (i.e. guided).

While ECC density increased progressively over 1 to 2 weeks in radial and sheet co-cultures, and in EC-only cultures, it fell by at least a half in axial co-cultures (see Supplementary results section). Mean ECC area was inversely correlated to ECC number, showing an increase on the surface of axial co-cultures (no ECCs in core region at 2 weeks) against a reduction, or no significant change, in all other conditions tested from 1 to 2 weeks. In combination, these findings would suggest that in axial co-cultures ECCs progressively fused to form larger aggregates or CLSs (in the core), but under all other conditions endothelial cells continued to form clusters with no significant change in cluster size.

3.2. Hypoxia-induced generation of angiogenic factors

Previous work by this group has shown a dramatic upregulation of VEGF gene expression under physiological hypoxia in the core of 3D HDF-collagen constructs, over 8 days [5]. EC-only cultures and HIS-HDF/EC axial co-cultures were compared, in terms of expression of key angiogenic factors at the protein level (HIF1 α and VEGF), either secreted in the media or retained within the constructs over the 5–10 day culture period. As expected no HIF1 α (a nuclear transcription factor) was detected in any of the media, but was present within HIS-HDF/EC co-culture constructs, though there was no significant difference between 5 and 10 days (see Supplementary results section). Importantly, HIF1 α was not detectable within EC-only constructs, indicating that the ECs were not directly under hypoxia. VEGF was found in both media and constructs of HIS-HDF/EC co-cultures, at 5 and 10 days, showing VEGF retention within these collagen scaffolds (Fig. 2). VEGF retention: release ratio was approximately 3:1 (construct : medium) at 10 days. While VEGF protein levels increased from 5 to 10 days culture, this increase (7-fold) was statistically significant only for constructs ($p < 0.05$). This was consistent with increasing VEGF gene expression over 8 days [5]. No VEGF was detectable in EC-only cultures, at both 5 and 10 days (Fig. 2), which was in agreement with the absence of HIF1 α expression.

3.3. Reversal of HIS-mediated angiogenic response

The basic hypothesis here suggests that blocking the function of one of the key angiogenic factors (e.g. VEGF) would reverse the

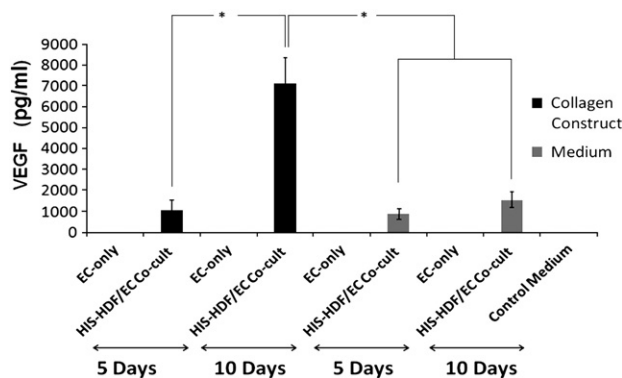


Fig. 2. Localized exposure of HDFs to physiological hypoxia resulted in up-regulation of VEGF protein expression *in vitro*. Elisa was used to analyse levels of VEGF protein secreted in the media or retained within collagen constructs of either EC-only cultures (1.16×10^6 HUVECs/ml) or HIS-HDF/EC axial co-cultures (23.2×10^6 HDFs/ml and 1.16×10^6 HUVECs/ml) at 5 and 10 days. VEGF was produced into both collagen constructs and media, though not by ECs. Basal (zero) control medium was DMEM supplemented with 5% FCS. Bars correspond \pm sd of means, $*p < 0.05$. Three samples ($n = 3$) were analysed for each condition tested per time point.

cellular angiogenic response to hypoxia-induced signaling in this 3D system. Ability to block the *HIS* angiogenic response was tested in *HIS*-HDF/EC axial co-cultures pre-incubated with either non-specific IgG or anti-VEGF neutralizing IgG. Anti-VEGF treatment did not affect the standard response in terms of number of CLSs formed within the *HIS*-HDF compartment (either core or surface at 1 week, data not shown). However, Fig. 3 shows that anti-VEGF treatment did reduce the mean length of CLSs formed within the *HIS*-HDF compartment. While this inhibition of function was seen in both the core and surface zones compared to non-specific IgG controls, at 1 week, the difference was only significant on the surface ($p < 0.05$). This could be due to partial diffusion of antibody through the construct (filtration studies showed that at least 8% of IgG was retained per collagen layer of the spiral, unpublished data). The significant, but partial, abolition of function seen at the surface, where VEGF blockade was not limited (constructs incubated at saturating concentration of anti-VEGF IgG) indicated that anti-VEGF treatment was only partially effective in blocking the *HIS* mediated angiogenic response.

3.4. *In vivo* vascularization with *HIS* implants

We have previously reported vascular in-growth into 3D spiral collagen constructs by 3 weeks *in vivo* implantation, without angiogenic signalling [23]. We therefore tested if 3D constructs containing *HIS* fibroblasts would become vascularized earlier. The ability to further accelerate construct vascularisation by pre-upregulating angiogenic factor expression through *in vitro* pre-conditioning was also tested. Acellular or rabbit dermal fibroblast (RDF)-seeded collagen constructs were implanted subcutaneously into the back of rabbits. Cell-seeded constructs comprised of an outer acellular wrap and a *HIS*-RDF core (Fig. 4) at: (i) low cell density (5.8×10^6 RDFs/ml) 5-day pre-conditioned (LDPC), (ii) high cell density (23.2×10^6 RDFs/ml) 5-day pre-conditioned (HDPC) and (iii) high cell density (23.2×10^6 RDFs/ml) without pre-conditioning (HD). Total white blood cell count in rabbits implanted with cell-seeded constructs was 8.2, 15.5, 9.1, 5.5×10^9 cells/L on day 0, 1, 7 and 14 respectively, indicating subsidence of the inflammatory response by 7 days.

In contrast to acellular constructs, which showed no visible vascularisation at 1 week, LDPC, HDPC and HD constructs were all grossly vascularised by 1 week *in vivo* (Fig. 4A). Importantly, host vessels invading the collagen constructs at 1 week contained intraluminal red blood cells (RBCs), suggesting that these vessels were functional by 1 week (Fig. 4B). Furthermore, these vessels stained positively with anti-CD31 (Fig. 4B). LDPC constructs had the largest total area of invading RBC-containing vessels at 1 week (10 fold greater than acellular controls; $p < 0.05$), and HDPC constructs the least (Fig. 4C). Although there were differences in vascularisation

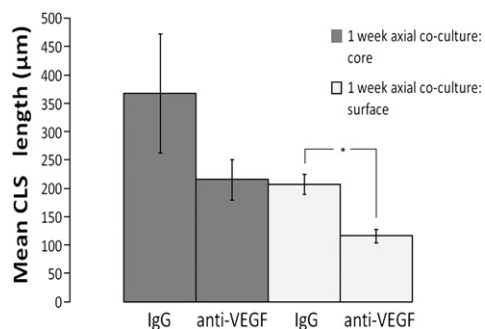


Fig. 3. Blocking the function of VEGF only partially abolished the angiogenic response to hypoxia-induced signalling. *HIS*-HDF/EC axial co-cultures were incubated with either non-specific IgG or anti-VEGF IgG, at saturating concentration (10 µg/ml), for 1 week and the length of CD31 +ve CLSs within the HDF compartment was analysed for the core and surface zones separately. Bars correspond \pm se of means, * $p < 0.05$. Four constructs ($n = 4$) were tested for each condition.

rates between types of cellular constructs, these did not reach statistical significance ($p > 0.05$). There was an overall increase in the total area of RBC-containing host vessels in all implanted constructs, including acellular constructs, by 2 weeks post-implantation, consistent with the anti-CD31 staining (Fig. 4B). While all cellular constructs showed greater vascularisation than acellular constructs at 2 weeks, this difference was smaller than at 1 week and not statistically significant ($p > 0.05$) (Fig. 4C). Radial invasion distance of host blood vessels permeating the collagen spirals was approximately 2 fold higher for cellular constructs compared to acellular constructs at 1 week (Fig. 4D). At 1 week blood vessels had only penetrated into the acellular wrap (~0.77 mm thickness) in cell-seeded constructs, without reaching the cellular core (Fig. 4D). Acellular construct vascularisation had caught up by 2 weeks, though by this stage some host blood vessels had penetrated into the core of LDPC and HD constructs (Fig. 4D).

In vivo vessel functionality was assessed by real-time monitoring of core O_2 levels in acellular and RDF-seeded spiral constructs, implanted intramuscularly over 2 weeks. Cellular constructs seeded at low density (LD: 5.8×10^6 RDFs/ml) or high density (HD: 23.2×10^6 RDFs/ml) were implanted directly without *in vitro* pre-conditioning. By 2 weeks host vessels containing intra-luminal RBCs were present in acellular, LD and HD constructs, although both types of cellular constructs were more profoundly perfused than acellular constructs (Fig. 5A). Initial (immediately post surgery) core O_2 levels of LD and HD constructs were approximately 30% ($p > 0.05$) and 90% ($p < 0.001$) less than acellular constructs, respectively (Fig. 5B). However, while core O_2 levels of acellular constructs continued to drop over the whole 2 weeks (due, in part at least, to inflammatory and connective tissue host cell infiltration [23]) core O_2 levels of LD constructs leveled off at a min (5–10 mm Hg) by day 3. Two week core O_2 levels in LD constructs were 4 fold higher than those of acellular constructs. This correlated with a 2 fold greater area of RBC-containing vessels in LD constructs compared to acellular constructs (Fig. 5C). Core O_2 levels in HD constructs remained low in the first 5 days (due to their seeded cell O_2 consumption), but increased 5 fold by 1 week. This high level of core O_2 (12–15 mm Hg) was maintained over the second week, leaving the HD construct core O_2 2 and 10 fold greater than LD and acellular constructs, respectively, at 2 weeks. The difference between total area of RBC-containing vessels in HD and acellular constructs was not significant ($p > 0.05$, Fig. 5C), despite the significant difference in core O_2 levels at 2 weeks ($p < 0.05$, Fig. 5B).

4. Discussion

The well recognized principle of complex spatio-temporal/chemical co-ordination in angiogenesis [9,24] was highlighted here in the finding that functional blocking of VEGF only partially abolished the *HIS* angiogenic response *in vitro*. This has important implications for engineering angiogenesis. Indeed, trying to mimic the necessary physiological complexity using bottom-up engineering of angiogenic cocktails appears to be near insurmountable at our current level of understanding [24–26]. A clear alternative is to engineer the onset of the process by producing local hypoxia (which is easier to control) in engineered cell populations to upregulate hypoxia-induced signaling (i.e. a physiological angiogenic cascade). The problem then shifts from trying to mimic a complex chemical language to engineering a predictable local cell-hypoxia.

Exposure of cells to physiological hypoxia has been shown to be effective in activating the production of cell-generated angiogenic factors [5,6,27]. In this study we have demonstrated that O_2 consumption by a high density depot of normal HDFs generated a self-sustaining *HIS* cell response leading to the production of a functional sequence of critical angiogenic factor proteins. While physiological regulation of the O_2 microenvironment in this system maintained a high cell viability (>80%) up to 5 days, some level of *HIS*

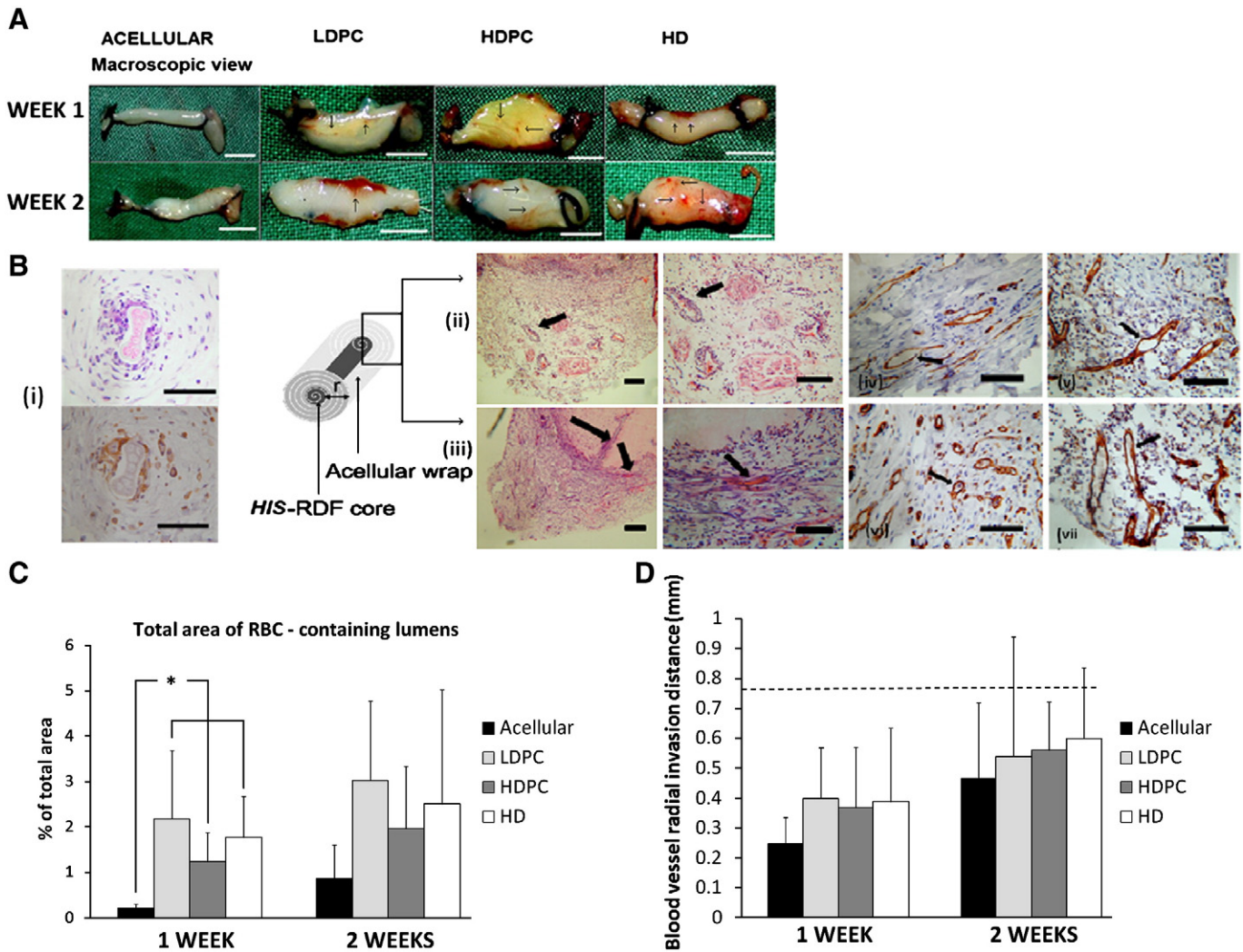


Fig. 4. Hypoxia-induced signalling *in vivo* promoted rapid vascularization of cellular constructs. (A) Collagen constructs +/– RDF seeding were sutured subcutaneously in rabbits for 1 or 2 weeks. Cell-seeded constructs were low density pre-conditioned (LDPC), high density pre-conditioned (HDPC) and high density non-pre-conditioned (HD). Macroscopic images were taken directly after implant recovery. Arrows indicate host vessels that had infiltrated the implants (bars = 0.5 cm). (B) (i) Co-localisation of H&E staining (top panel) with CD31 (bottom panel) in a 2 week HDPC construct. H&E staining (arrows indicate magnified areas): (ii) Transverse section of 1 week HDPC construct with magnification image. Schematic indicates the corresponding plane within the construct. (iii) Transverse section of 2 week HDPC construct with magnification image. Long arrow indicates penetration of cells towards the construct core. CD31 staining counterstained with haematoxylin, arrows indicate CD31 +ve endothelial cells lining vessel lumens: (iv) Positive control-muscle from rabbit. (v) 1 week LDPC construct. (vi) 1 week HDPC construct. (vii) 2 week LDPC construct (bars = 100 μ m). (C) Quantification of the total area of RBC-containing lumens (H&E stained cross sections, as percentage of total section area) in subcutaneously implanted constructs, at 1 and 2 weeks. (D) Quantification of host blood vessel radial invasion distance for all conditions tested. Dashed line indicates the distance (0.77 mm) from the construct surface to the cellular core. Bars correspond to \pm sd of means, * $p < 0.05$. Six constructs ($n = 6$) were tested for each condition.

cell damage or death is expected over longer culture periods [5]. It is important to note, however, that metabolic products released from hypoxic tissues (e.g. lactate, pyruvate, adenosine, malate) have been reported to be intermediate effectors of angiogenesis [28], rather than inhibit the process. *In vitro* ECs migrated and formed tubules towards the source of angiogenic factors (*HIS* cells) by 1 week. In contrast to other co-cultured (2D) models with mixed cell populations [19,29,30], this model enables the spatial segregation of distinct directing and responder cell populations to test the effect of contact-independent cell signaling i.e., endothelial cell migration/tubule formation along an angiogenic growth factor gradient (note: the stability of cell segregation in this model was achieved by the large separation distance (1.5 cm) between the cell compartments and the retardation of fibroblast migration in compressed/dense collagen matrix [31]). The ability to spatially position *HIS* cells within a 3D construct also means that exposure of endothelial cells to cell-generated hypoxia (and its negative impact on cell viability[32]) is avoided, which would not be possible with mixed co-culture.

Importantly, this novel seeding technique lays the foundation for developing endothelial cell-free angiogenic implants (tested here *in vivo*), eliminating cell source limitations and ethical considerations. The absence of angiogenic responses in both EC-only cultures and sheet co-cultures (no hypoxia) demonstrates the need for hypoxia-induced signaling, rather than simple presence of HDFs. Although readily available HDFs were used for *HIS* generation, for simplicity, work from this group and others has shown that multiple cell types (e.g. bone marrow-derived stromal cells, vascular smooth muscle cells) respond to physiological hypoxia by upregulating angiogenic signaling [12,15,16,33,34], suggesting that different cell types could be used as the source of *HIS* cells, provided that cells are exposed to optimum (i.e. cell-type specific) levels of physiological hypoxia [5,16]. It is likely then that this mechanism of engineered angiogenesis can be adapted to many tissues.

The target of this study was to test and evaluate the ability of *HIS* cells, controlled using a model engineered tissue, to induce effective vascularisation. Importantly, a collagen type I support material was

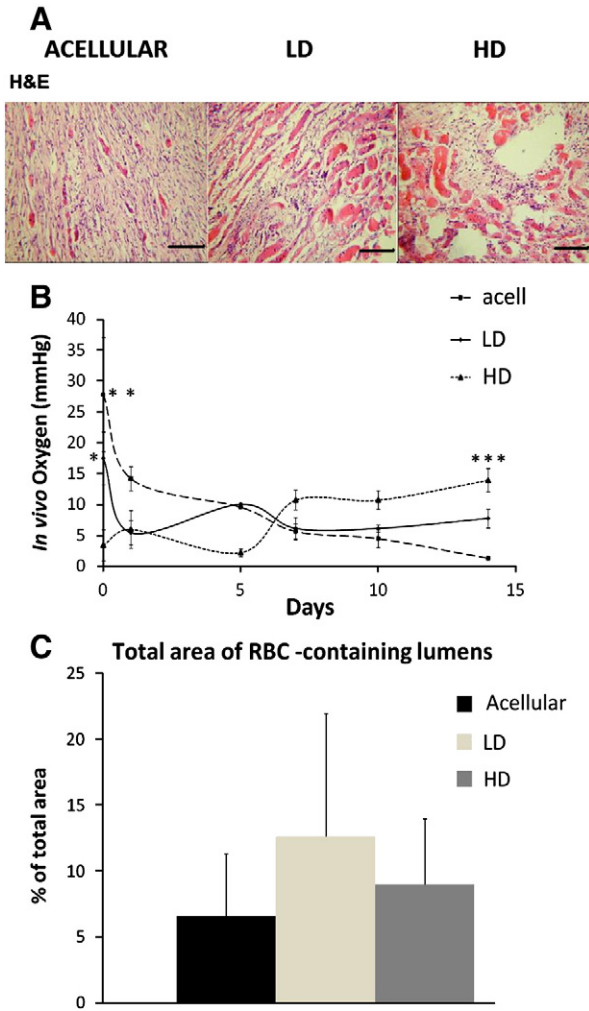


Fig. 5. Assessment of the functionality of invading host blood vessels into implanted constructs by real-time monitoring of O₂ levels *in vivo*. (A) Vascularization of intramuscularly implanted constructs; acellular, low density (LD), high density (HD) after 2 weeks implantation. Construct tissue sections stained with H&E show clear increase in RBC-filled vessel lumens in both types of cellular constructs (bars = 100 μm). (B) Real-time O₂ tension in the core of intramuscularly implanted constructs over 2 weeks implantation. Results are presented as partial pressure values (pO₂) in mm Hg. Time zero values represent readings taken in constructs immediately after implantation. Bars correspond +/- se of means, *p<0.01 (HD vs. LD at day 0), **p<0.001 (HD vs. acellular at day 0), ***p<0.05 (HD vs. acellular at day 14). Three constructs were tested for each condition. (C) Quantification of the total area of RBC-containing lumens (H&E stained cross sections, as percentage of total section area) in acellular, LD and HD constructs after 2 weeks implantation. Bars correspond to +/- sd of means). Three constructs (n = 3) were tested for each condition.

used to ensure a biomimetic tissue microenvironment [21]. The predictive importance of the 3D collagen model for practical, precise operation of the engineered angiogenesis cannot be overemphasized. It is clearly possible to use the demonstration of hypoxia-induced angiogenesis by simply packing a large number of cells deep into any 3D construct. However, while this is eventually likely to generate some form of angiogenic growth factor cascade, it is actually of very limited practical significance without precision and control. The key new element here is that it is possible in principle, not only to predict and tune when the angiogenic burst is released, but to what extent, how long for and most importantly, where from. The anisotropy of the 3D collagen model reflects the anisotropy found in almost all native tissues. There are two levels of important anisotropy. The first and least obvious, lies in the ability for small molecules (e.g. oxygen, glucose, lactate) to diffuse rapidly in most directions through the collagen nano-fibre mesh, even at high collagen densities [5,35]. Therefore, in spiral

constructs O₂ tension is almost entirely determined by cell O₂ consumption [15]. Importantly, we previously showed that the generated O₂ consumption gradient (core O₂<surface O₂) correlates with greater VEGF gene expression in the core compared to the surface [5]. A functional output of this anisotropic effect was the stronger angiogenic response observed in the core vs. the surface of *HIS*-HDF/EC axial co-cultures at 2 weeks. The second level of anisotropy relates to the diffusion of macromolecules. Since these have longer transit times through the nano-porous collagen mesh, the direction and magnitude of macromolecular (e.g. angiogenic factor protein) gradients will mainly be determined by the diffusive properties of the matrix [36]. In spiral collagen constructs macromolecule diffusion would predominantly occur along the path of least resistance i.e. primarily between collagen matrix layers, with slower diffusion through layers. In axial model co-cultures this would generate a strong axial angiogenic factor gradient from the *HIS*-HDFs to the ECs, while in radial model co-cultures the presence of this diffusion barrier would reduce the radial angiogenic factor gradient established between the two cell populations (Fig. 6). This could, at least partly, explain why a greater CLS score was obtained in axial model co-cultures (core) than in radial model co-cultures at 2 weeks.

EC migration has previously been observed in response to gradients of VEGFA 165 [8]. In the present system far more HIF-1α and VEGF was generated in the *HIS*-HDF compartment than the EC compartment, where growth factor proteins were undetectable (as demonstrated in the EC-only cultures). This expression correlated closely with the larger number of CLSs formed in the *HIS*-HDF compartment than in the EC compartment at 2 weeks (core of axial co-cultures). In contrast, CLS length was influenced primarily by the spatial position of ECs relative to *HIS* cells in the spiral. In axial model co-cultures, where ECs were aligned with the axial angiogenic factor gradient (Fig. 6), longer CLSs formed in the EC compartment than in the *HIS*-HDF compartment, i.e. furthest away from the growth factor source, at 2 weeks. This is consistent with ECs forming tubular structures back along a gradient, towards its source. Importantly, in radial model co-cultures, where protein growth factors had to cross the low permeability collagen layers (i.e. a diffusion barrier) to reach the responder ECs, CLSs in the EC compartment were shorter. The proposed generation of angiogenic factor gradients in this system, then, seems to recapitulate the native tissue in that the effects of protein factors are superimposed (sometimes dominated) by the matrix 3D structure and its enabling or restricting effects on growth factor diffusion [37]. In contrast to CLS formation ‘clustering’ appeared to be an intrinsic EC behavior rather than a response to hypoxia and

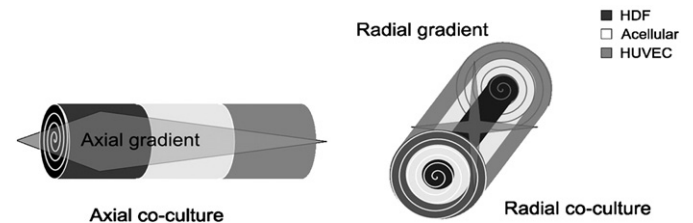


Fig. 6. Schematic showing the proposed 3D spatial organisation of angiogenic factor gradients in the *in vitro* model used to investigate the induction of angiogenesis by hypoxia-induced signalling. In spiral collagen constructs, diffusion of macromolecules (i.e. angiogenic factor proteins), produced by *HIS* cells (HDFs), is predicted to follow predominantly the path of least resistance, primarily between collagen matrix layers. Diffusion will be far slower through the layers. Based on this analysis, in *HIS*-HDF/EC axial co-cultures (left panel) a strong axial angiogenic factor gradient would be generated from the *HIS* cells at one end to the ECs at the other (i.e. between the spiral layers). However, in *HIS*-HDF/EC radial co-cultures (right panel) a much smaller diffusion gradient would be expected to develop between the two cell populations, limited by the reduced protein diffusion rate through the dense collagen layers. This prediction, tested here, suggests that spatially-defined, biomimetic depot-release can be achieved, making it possible to direct the angiogenic gradient to a required 3D tissue position.

angiogenic protein generation, as previously suggested [29]. While there was minimal or no HIF-1 α and VEGF accumulation in EC-only cultures up to 10 days, this did not prevent EC clustering. However, CLS formation only occurred where a *HIS*-HDF population was present, suggesting that whilst there may be a cluster-to-CLS transition, it critically depends on the presence of angiogenic factors to progress all the way to CLS formation.

HIS cell-generated *in vivo* angiogenesis was achieved within 1 week compared to studies where scaffold vascularisation by exogenous delivery of growth factor cocktails takes a minimum of 2 weeks [24–26]. This time delay is critical for implanted tissues, inevitably governing their dimensions and success rate [38]. *HIS* cell-generated growth factor production, in the present study, successfully accelerated the formation of functional vessels *in vivo* by 1 week. The proposed mechanism is recapitulation of angiogenic sprouting from the host, as it is known that sprouts are formed from existing vasculature in response to gradients of angiogenic proteins from avascular (as in this model) or ischaemic tissue [13]. A previous study by this group showed that a minimum of 3 weeks is required for functional vascularisation of low cell density implants [23]. The present study showed that even these low cell density constructs have enhanced vascularisation (by 1 week) when pre-conditioned for 5 days *in vitro*, to optimally up-regulate angiogenic signaling [5]. Other groups have reported that hypoxic pre-conditioning of implanted bone marrow cells increases their angiogenic potency through up-regulation of VEGF expression [33]. This might have important implications for use of hypoxic pre-conditioning as an additional strategy to vascularise *HIS* cell-seeded constructs post-implantation. In our model there was no histomorphometric improvement of angiogenesis *in vivo* using high cell density constructs, suggesting that an angiogenic factor cascade is generated at threshold O₂ levels or that *in vivo* there is a maximum speed of response, independent of growth factor levels. This has practical, bio-processing importance where cell availability is a limiting factor.

Real time measurement of changing *in vivo* local O₂ levels, deep inside the implant, is probably the most effective/relevant functional outcome of angiogenic engineering currently available. This provides direct readout of the integration and likely survival of constructs [39], making close analysis of the core O₂ data particularly important. While core O₂ tension was initially determined by resident (seeded) cell consumption, competition for O₂ (and likely other nutrients, not measured here) between implant and native tissue became increasingly dominated by surrounding/in-growing host cell consumption, as shown by the acellular construct baseline which dropped below that of cellular constructs by 5–7 days. Furthermore, since there was clear histological evidence of greater infiltration of RBC filled vessels in 14 day LD and HD constructs than in acellular constructs, it is probable that the 4 and 10 fold difference in core O₂ at day 14, respectively, was due to increased vascular perfusion. Histological analysis demonstrated that there was some level of cell death within LD and HD constructs, indicated by the presence of cell sparse areas (especially in the core, data not shown), by 2 weeks implantation. However, since cell death is hypoxia-driven, it cannot have exceeded the acellular construct baseline, confirming the histological data which suggest that the higher 14 day O₂ levels measured within cell-seeded constructs were a result of increased vascularisation and not reduced cell O₂ consumption. These results further indicate that the *HIS* response was sustained long enough for effective angiogenic induction. While it is intended that rapid vascularization of native tissue surrounding the implant will also rescue the *HIS* cell depot, maintaining angiogenic signaling, further *in vivo* work is required to identify the precise effect of initial nutrient deprivation on *HIS* cell viability. Importantly, the O₂ level obtained in HD implants at 14 days (~15 mm Hg/2%) was near the range reported for normal muscle

(20–30 mm Hg/2.6–3.9%) [40], indicating that the implants had at least partially integrated with the host tissue.

5. Conclusions

While it is widely accepted that long-term exposure of cells to hypoxia can be detrimental to cell viability, the results of this study demonstrate for the first time that spatially controlled, cell-mediated hypoxia can be employed as a stimulus to trigger the complete angiogenic cascade for induction of a rapid, physiological angiogenic response *in vitro* and *in vivo*. The control and predictability of this system means that this can genuinely claim to be engineered angiogenesis. Indeed, the system not only allows the timed switching 'on' of local angiogenesis, but also its spatial location and even direction. Our findings suggest that while it might not yet be possible to contain the extent of engineered 'on-off' angiogenesis *in vivo* (as assessed by histological appearance), this system can be used to successfully engineer early functional vascular perfusion of implants, as seen by deep tissue oxygenation. The ability to spatially localize *HIS* cells within a 3D tissue construct provides a powerful tool for tissue modeling *in vitro* (e.g. tumour angiogenesis [41], drug testing [19]), as well as pre-vascularization or pre-conditioning of engineered constructs for improving perfusion post-implantation [42]. Furthermore, the system is sufficiently flexible and robust to form the platform for a range of practical angiogenic therapies. A key strength of this study is the correlation of engineered angiogenesis with *in vivo* O₂ monitoring. This is a powerful indicator of successful construct vascularization, survival and integration. Assessment of O₂ and nutrient delivery to any implanted tissue forms the ultimate test of the ability of an engineered vasculature to function effectively.

Acknowledgements

Umber Cheema is a funded BBSRC David Phillips Fellow. We are grateful to BBSRC/EPSC and the China Partnering Award. We would like to thank Michael Ananta for their help with the schematic illustrations and staining, and Huiguo Chu for help with surgery.

Appendix A. Supplementary data

Supplementary data associated with this article can be found, in the online version, at doi:10.1016/j.jconrel.2010.05.037.

References

- [1] V. Falanga, R.S. Kirsner, Low oxygen stimulates proliferation of fibroblasts seeded as single cells, *J. Cell. Physiol.* 154 (1993) 506–510.
- [2] B. Annabi, Y.T. Lee, S. Turcotte, E. Naud, R.R. Desrosiers, M. Champagne, N. Eliopoulos, J. Galipeau, R. Beliveau, Hypoxia promotes murine bone-marrow-derived stromal cell migration and tube formation, *Stem Cells* 21 (2003) 337–347.
- [3] T. Ma, S.T. Yang, D.A. Kniss, Oxygen tension influences proliferation and differentiation in a tissue-engineered model of placental trophoblast-like cells, *Tissue Eng.* 7 (2001) 495–506.
- [4] K.M. Okazaki, E. Maltepe, Oxygen, epigenetics and stem cell fate, *Regen. Med.* 1 (2006) 71–83.
- [5] U. Cheema, R.A. Brown, B. Alp, A.J. MacRobert, Spatially defined oxygen gradients and vascular endothelial growth factor expression in an engineered 3D cell model, *Cell. Mol. Life Sci.* 65 (2008) 177–186.
- [6] A. Namiki, E. Brogi, M. Kearney, E.A. Kim, T.G. Wu, T. Couffinhal, L. Varticovski, J.M. Isner, Hypoxia induces vascular endothelial growth factor in cultured human endothelial cells, *J. Biol. Chem.* 270 (1995) 31189–31195.
- [7] G.L. Semenza, Hypoxia-inducible factor 1: master regulator of O-2 homeostasis, *Curr. Opin. Genet. Dev.* 8 (1998) 588–594.
- [8] I. Barkefors, S. Le Jan, L. Jakobsson, E. Hejll, G. Carlsson, H. Johansson, J. Jarvius, J.W. Park, N.L. Jeon, J. Kreuger, Endothelial cell migration in stable gradients of vascular endothelial growth factor a and fibroblast growth factor 2 – effects on chemotaxis and chemokinesis, *J. Biol. Chem.* 283 (2008) 13905–13912.
- [9] P. Carmeliet, Mechanisms of angiogenesis and arteriogenesis, *Nat. Med.* 6 (2000) 389–395.
- [10] P. Fraisl, M. Mazzone, T. Schmidt, P. Carmeliet, Regulation of angiogenesis by oxygen and metabolism, *Dev. Cell* 16 (2009) 167–179.

- [11] I. Papandreou, A. Powell, A.L. Lim, N. Denko, Cellular reaction to hypoxia: sensing and responding to an adverse environment, *Mutat. Res.* 569 (2005) 87–100.
- [12] J. Rouwkema, N.C. Rivron, C.A. van Blitterswijk, Vascularization in tissue engineering, *Trends Biotechnol.* 26 (2008) 434–441.
- [13] G.D. Yancopoulos, S. Davis, N.W. Gale, J.S. Rudge, S.J. Wiegand, J. Holash, Vascular-specific growth factors and blood vessel formation, *Nature* 407 (2000) 242–248.
- [14] L. Coultas, K. Chawengsaksophak, J. Rossant, Endothelial cells and VEGF in vascular development, *Nature* 438 (2005) 937–945.
- [15] U. Cheema, E. Hadjipanayi, N. Tammi, B. Alp, V. Mudera, R.A. Brown, Identification of key factors in deep O₂ cell perfusion for vascular tissue engineering, *Int. J. Artif. Organs* 32 (2009) 318–328.
- [16] H. Sakuda, Y. Nakashima, S. Kuriyama, K. Sueishi, Media conditioned by smooth muscle cells cultured in a variety of hypoxic environments stimulates in vitro angiogenesis. A relationship to transforming growth factor-beta 1, *Am. J. Pathol.* 141 (1992) 1507–1516.
- [17] J. Ke, Y. Liu, X. Long, J. Li, W. Fang, Q. Meng, Y. Zhang, Up-regulation of vascular endothelial growth factor in synovial fibroblasts from human temporomandibular joint by hypoxia, *J. Oral Pathol. Med.* 36 (2007) 290–296.
- [18] C.K. Griffith, S.C. George, The effect of hypoxia on in vitro prevascularization of a thick soft tissue, *Tissue Eng. Part A*, 2009.
- [19] P.L. Tremblay, F. Berthod, L. Germain, F.A. Auger, In vitro evaluation of the angiostatic potential of drugs using an endothelialized tissue-engineered connective tissue, *J. Pharmacol. Exp. Ther.* 315 (2005) 510–516.
- [20] Z. Chen, A. Htay, S.W. Dos, G.T. Gillies, H.L. Fillmore, M.M. Sholley, W.C. Broadus, In vitro angiogenesis by human umbilical vein endothelial cells (HUVEC) induced by three-dimensional co-culture with glioblastoma cells, *J. Neurooncol.* 92 (2009) 121–128.
- [21] R.A. Brown, M. Wiseman, C.B. Chuo, U. Cheema, S.N. Nazhat, Ultrarapid engineering of biomimetic materials and tissues: fabrication of nano- and microstructures by plastic compression, *Adv. Funct. Mater.* 15 (2005) 1762–1770.
- [22] F.W. Lusinskas, J. Lawler, Integrins as dynamic regulators of vascular function, *FASEB J.* 8 (1994) 929–938.
- [23] V. Mudera, M. Morgan, U. Cheema, S. Nazhat, R. Brown, Ultra-rapid engineered collagen constructs tested in an in vivo nursery site, *J. Tissue Eng. Regen. Med.* 1 (2007) 192–198.
- [24] N.C. Rivron, J.J. Liu, J. Rouwkema, B.J. de, C.A. van Blitterswijk, Engineering vascularised tissues in vitro, *Eur. Cell Mater.* 15 (2008) 27–40.
- [25] S.T. Nillesen, P.J. Geutjes, R. Wismans, J. Schalkwijk, W.F. Daamen, T.H. van Kuppevelt, Increased angiogenesis and blood vessel maturation in acellular collagen-heparin scaffolds containing both FGF2 and VEGF, *Biomaterials* 28 (2007) 1123–1131.
- [26] T.P. Richardson, M.C. Peters, A.B. Ennett, D.J. Mooney, Polymeric system for dual growth factor delivery, *Nat. Biotechnol.* 19 (2001) 1029–1034.
- [27] M.W. Laschke, Y. Harder, M. Amon, I. Martin, J. Farhadi, A. Ring, N. Torio-Padron, R. Schramm, M. Rucker, D. Junker, J.M. Haufel, C. Carvalho, M. Heberer, G. Germann, B. Vollmar, M.D. Menger, Angiogenesis in tissue engineering: breathing life into constructed tissue substitutes, *Tissue Eng.* 12 (2006) 2093–2104.
- [28] B. Murray, D.J. Wilson, A study of metabolites as intermediate effectors in angiogenesis, *Angiogenesis* 4 (2001) 71–77.
- [29] M. Raghunath, Y.S. Wong, M. Farooq, R. Ge, Pharmacologically induced angiogenesis in transgenic zebrafish, *Biochem. Biophys. Res. Commun.* 378 (2009) 766–771.
- [30] S. Levenberg, J. Rouwkema, M. Macdonald, E.S. Garfein, D.S. Kohane, D.C. Darland, R. Marini, C.A. van Blitterswijk, R.C. Mulligan, P.A. D'Amore, R. Langer, Engineering vascularized skeletal muscle tissue, *Nat. Biotechnol.* 23 (2005) 879–884.
- [31] E. Hadjipanayi, R.A. Brown, V. Mudera, Interface integration of layered collagen scaffolds with defined matrix stiffness: implications for sheet-based tissue engineering, *J. Tissue Eng. Regen. Med.* 3 (2009) 230–241.
- [32] A. Stempien-Otero, A. Karsan, C.J. Cornejo, H. Xiang, T. Eunson, R.S. Morrison, M. Kay, R. Winn, J. Harlan, Mechanisms of hypoxia-induced endothelial cell death. Role of p53 in apoptosis, *J. Biol. Chem.* 274 (1999) 8039–8045.
- [33] T.S. Li, K. Hamano, K. Suzuki, H. Ito, N. Zempo, M. Matsuzaki, Improved angiogenic potency by implantation of ex vivo hypoxia prestimulated bone marrow cells in rats, *Am. J. Physiol. Heart Circ. Physiol.* 283 (2002) H468–H473.
- [34] S.C. Hung, R.R. Pochampally, S.C. Chen, S.C. Hsu, D.J. Prockop, Angiogenic effects of human multipotent stromal cell conditioned medium activate the PI3K-Akt pathway in hypoxic endothelial cells to inhibit apoptosis, increase survival, and stimulate angiogenesis, *Stem Cells* 25 (2007) 2363–2370.
- [35] Z.M. Rong, U. Cheema, P. Vadgama, Needle enzyme electrode based glucose diffusivity transport measurement in a collagen gel and validation of a simulation model, *Analyst* 131 (2006) 816–821.
- [36] E.M. Johnson, D.A. Berk, R.K. Jain, W.M. Deen, Hindered diffusion in agarose gels: test of effective medium model, *Biophys. J.* 70 (1996) 1017–1023.
- [37] L. Lamallice, F. Le Boeuf, J. Huot, Endothelial cell migration during angiogenesis, *Circ. Res.* 100 (2007) 782–794.
- [38] C.K. Griffith, C. Miller, R.C.A. Sainson, J.W. Calvert, N.L. Jeon, C.C.W. Hughes, S.C. George, Diffusion limits of an in vitro thick prevascularized tissue, *Tissue Eng.* 11 (2005) 257–266.
- [39] W. Wang, P. Vadgama, O₂ microsensors for minimally invasive tissue monitoring, *J. R. Soc. Interface* 1 (2004) 109–117.
- [40] C. Baudelet, B. Gallez, Effect of anesthesia on the signal intensity in tumors using BOLD-MRI: comparison with flow measurements by laser Doppler flowmetry and oxygen measurements by luminescence-based probes, *Magn. Reson. Imaging* 22 (2004) 905–912.
- [41] D. Shweiki, M. Neeman, A. Itin, E. Keshet, Induction of vascular endothelial growth factor expression by hypoxia and by glucose deficiency in multicell spheroids: implications for tumor angiogenesis, *Proc. Natl. Acad. Sci. USA* 92 (1995) 768–772.
- [42] E.A. Phelps, A.J. Garcia, Update on therapeutic vascularization strategies, *Regen. Med.* 4 (2009) 65–80.